v. 3, n. 58, 2023

International Journal of Health Science

DENTAL RESTORATION WITH OCCLUSAL ISLAND: A FINITE ELEMENT METHOD STUDY

Edgard Poiate Junior
Universidade do Estado do Rio de Janeiro,
Instituto Politécnico
Nova Friburgo – RJ
https://orcid.org/0000-0001-8937-4428

Raphael de Souza Ramalho Victor Ferreira
Universidade do Estado do Rio de Janeiro,
Instituto Politécnico
Nova Friburgo – RJ
http://lattes.cnpq.br/1672271560326680

Isis Andréa Venturini Pola Poiate
Universidade Federal Fluminense
Instituto de Saúde de Nova Friburgo,
Nova Friburgo – RJ
https://orcid.org/0000-0003-4721-5597

Abstract: When a posterior tooth has its functionality compromised, it must be repaired with a restorative material. In order to verify the potential use of types of occlusal islands for the recovery of regions in occlusal contact, the present study compared the stress distribution when applying a central load of 291.36 N, simulating centric bruxism (BC), in a healthy maxillary 2nd premolar tooth (HC), with a Class 1 restoration in Filtek bulk fill posterior resin without (RC) and with (RICC) occlusal islands in Vita Enamic hybrid ceramic in two regions of occlusal contact in cusps. BC loading was also compared on the supporting cusp of a healthy mandibular second premolar (HV) with a sloped restoration in Filtek posterior bulk fill resin (RV) and in Vita Enamic hybrid ceramic (ICV). The MSC.Patran program was used in the construction of the six finite element models, the processing was carried out in the MSC.Nastran, and the von Mises stress distribution, principal maximum and maximum shear stress were evaluated. The RC and RICC models in relation to the HC reduced the tensile stresses in the remaining enamel and at the enamel/resin interface, but caused an increase in the tensile stresses in the region between the islands. The ICV model compared to the RV model reduced the tensile stresses in the remaining enamel and in the island/enamel interface. It is concluded that in Class I restorations, the use of an occlusal island made of Vita Enamic hybrid ceramic on cusps and housed in Filtek bulk fill resin or the use of an occlusal island in a slope produces a beneficial effect on the longevity of the dental restoration in regions in occlusal contact injured by BC when the tooth is the upper or lower 2nd premolar, respectively. Therefore, the occlusal island can function as a sacrificial element, preserving the other structures, while there is no definitive solution for the patient's BC.

Keywords: Centric bruxism. Filtek bulk fill posterior. Finite Element Method. Restoration. Vita Enamic.

INTRODUCTION

When a posterior tooth has its functionality compromised by caries, excessive wear or fracture, it must be repaired with a restorative material (VASCONCELLOS et al., 2011).

Composite resins are usually chosen for this application due to their ease of handling, aesthetic characteristics, cost and mechanical performance. Its durability can exceed 10 years of service under ideal conditions, but in the presence of parafunctional habits such as biting objects, grinding teeth or constantly supporting the jaw with the hands, this useful life tends to decrease. Therefore, replacement of restorations due to mechanical failure is still one of the most common dental procedures (MUCELIN, 2015; ÁSTVALDSDÓTTIR, A. et al. 2015).

In 2011, a patent was registered at the National Institute of Intellectual Property (INPI), and granted in 2021, proposing to increase the durability of dental restorations and recover occlusal contacts from the installation of dental islands. Such islands consist of blocks of predefined geometry, capable of replacing missing dental elements or that have lost functionality and can also be installed in natural teeth or on other previously placed restorations, without requiring their complete removal (VASCONCELLOS et al., 2011).

Thus, the present work proposed to evaluate the distribution of stresses, strain and displacements in two types of restorations with an occlusal island inserted in an upper second premolar and a lower one, one type of island on the cusps subjected to central loading and the other in the vertex subjected to apex loading, respectively. And also, to compare their results to the respective healthy

or resin-restored teeth, with the application of a static load of centric bruxism, through the Finite Element Method, to verify the potential in the use of occlusal islands for the recovery of regions in occlusal contact.

LITERATURE REVIEW

Bruxism is a conscious or unconscious oral habit, characterized by non-functional contact between teeth (DUTRA, 2016), that is, friction, friction or clenching of the teeth, outside of normal functions (SERAIDARIAN, 2001).

According to its manifestation, it can be divided into eccentric bruxism (BE), defined by teeth grinding, and centric bruxism (BC), also known as tooth clenching (DUTRA, 2016; CHANTRE, 2019; DEMJAHA, 2019).

Both manifestations of bruxism are not considered a disease, but when the clinical picture becomes more pronounced, previously healthy teeth begin to show signs of wear in different degrees of intensity, which may exceed the dental enamel and generate large exposures of the dentin or lead to fracture (DUTRA et al, 2016).

Bartlett & Sundaram (2006) evaluated over 3 years in patients from London (England) the survival rate of composite resin restorations installed in posterior teeth (molars and premolars), which previously exhibited severe wear. At the end of the study, 50% of the restorations failed, while in the control group, the rate was 20%, indicating that in the presence of BC, resin restorations have a reduced survival rate.

This aspect becomes more critical during BC episodes, due to the high occlusion forces of the lower tooth with the upper one in a reduced contact area, resulting in significant compression and shear stresses, which may lead to an increase in tooth wear. Thus, the types of restorations selected for such patients must have high wear and fracture resistance to ensure the survival of the restoration and the tooth, but without neglecting the non-abrasive aspect with the antagonist tooth, given that the natural enamel must be preserved to the detriment of the restorative material (OSIEWICZ et al, 2019).

Another restorative option is dental ceramics, which reproduce most of the characteristics of natural teeth, especially compressive strength (MUCELIN, 2015) and color aesthetics. However, some features prevent its unrestricted use, such as its low fracture toughness, which may increase the probabilities of catastrophic failure of the restored tooth. The high hardness and modulus of elasticity contribute to increased wear of antagonist teeth, especially when combined with parafunctional habits such as bruxism (CESAR, 2018), in addition to the high cost and time to perform this type of restoration, which are higher in relation to the use of direct composite resin.

According to Gracis et al (2015), dental ceramics can be divided into three groups: ceramics with glass matrix, polycrystalline ceramics and ceramics with resin matrix or hybrid ceramics.

The so-called hybrid ceramic materials are actually composites consisting mostly of refractory inorganic compounds (ceramics), added to a polymer, which have become suitable for restoring areas with intense masticatory loads (VALJAKOVA et al, 2018).

The development of hybrid ceramics resulted in a material that has a mechanical behavior similar to that of hard dental tissues, with flexural strength superior to conventional composite resin, and capable of assimilating the resistance and fracture toughness of its matrix. And, they also have low rates of wear on the antagonist tooth compared to the wear caused by a restoration with other types of ceramics. (LUDOVICHETTI, 2018; VALJAKOVA et al, 2018;).

Commercially, hybrid ceramics are available in the form of blocks for CAD/CAM (Computer Aided Design / Computer Aided Manufacturing) to be milled by a CNC machining center, based on the geometry of the prepared tooth and its adjacent teeth, scanned and manipulated by a specific computer program. This technology allows for good accuracy in tooth repair, in addition to reducing patient stress by eliminating molding and reducing operative time, and there is no volumetric contraction of the material, when compared to the use of direct composite resin, since the resin contained in the block was previously polymerized (VALJAKOVA et al, 2018). However, it requires equipment (scanner and CNC), computer programs and a professional qualified in this technology, which generates a higher cost in the restoration in relation to the use of direct composite resin. This way, the installation of dental islands presents itself as a promising restorative method, increasing the durability of dental restorations and recovering occlusal contacts (VASCONCELLOS et al., 2011).

Dental islands are restorations with defined geometry and prefabricated, which can be used to restore a lost/damaged tooth under the occlusal contact area, that is, under contact points between opposing teeth, Figure 1a, and over ready-made restorations, in order to increase their longevity.

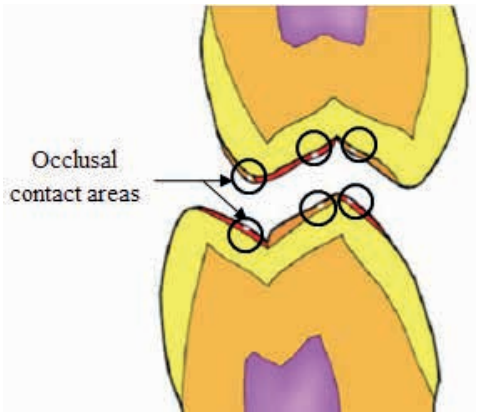

Figure 1a

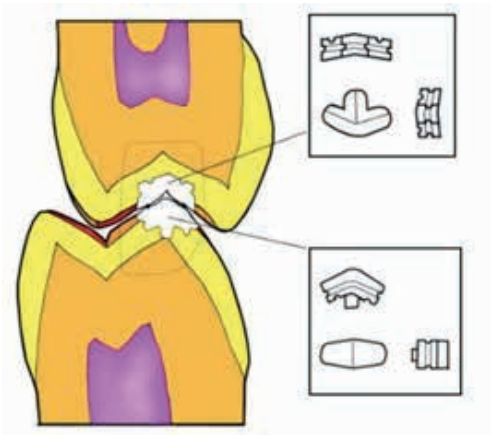

Figure 1b

Figure 1: a) Occlusal contact in premolar, b) Occlusal island in central fossa (upper tooth) and in cusp (lower tooth), Vasconcellos et al (2011).

Because they are prefabricated and because they do not require the removal of previously installed restorations, when placed over old restorations, the cost and operative time required are lower compared to the complete replacement of a restoration that has failed.

Its manufacturing method may also vary according to the selected material. Ceramics, metals, composites and resins can be used and, this way, the possible manufacturing processes become diverse, such as casting, sintering, molding and machining.

However, the site to be restored interferes with the choice of dental island, which is why there are three types: occlusal island, proximal island and occlusal cylindrical pin. In the present study, the occlusal cylindrical pin was applied on a Class I resin restoration, while the occlusal island was applied on the slope of the supporting cusp of the analyzed posterior tooth. The occlusal island is a type that can restore the cusp or central fossa of posterior teeth, also encompassing occlusal contact areas, Figure 1b.

When installed on the cusp, the installation begins with the removal of material corresponding to the area that will be replaced

by the occlusal island in the cusp. After this step, the area is chemically attacked, followed by the application of adhesive or dental cement, fixing the island, removing excesses and polishing.

In this work, the Finite Element Method (FEM) was used to evaluate the mechanical behavior in restorations with an occlusal island, indicating which areas are more likely to develop mechanical failures due to stress concentration (POIATE, 2007).

Mackerle (2004) presents a bibliography of more than 700 publications from 1990 to 2003 of the FEM widely used in several areas of dentistry, however, with greater application in the area of restorative dentistry, which studies the preservation and recovery of damaged, traumatized, defective or missing teeth.

Poiate et al (2011) performed a comparative analysis between 2D versus 3D modeling of a maxillary central incisor generated from computed tomography to show the importance of correct modeling of the physical problem.

MATERIAL AND METHODS

The geometry of the numerical model of the healthy tooth of the upper right 2nd premolar (tooth 15) developed by Poiate (2007), Figure 2, was the basis for the development of three geometric groups of models A, B and C, built in the MSC.Patran program version 2017.0. through the Finite Element Method (FEM).

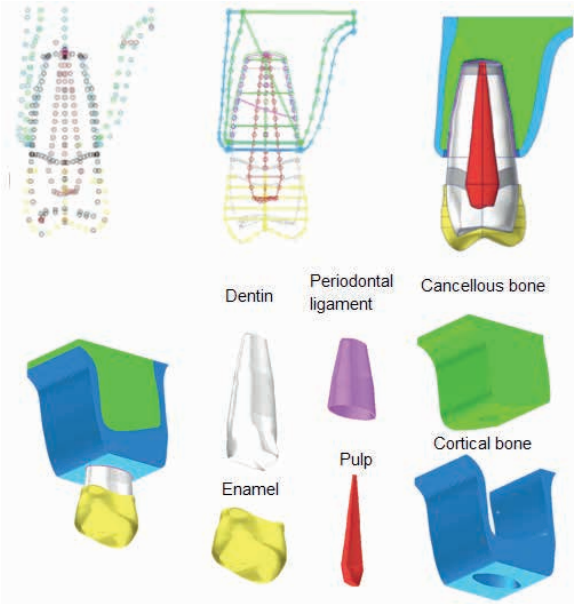

Figure 2: Modeling of healthy 2nd premolar, cortical and spongy bone (POIATE, 2007).

Geometry A, Figure 3a, corresponds to the healthy 2nd premolar of Poiate (2007), the tooth has a total length of 21.4 mm, root length of 14.1 mm, mesiodistal width of 5.0 mm and buccolingual width of 8.5 mm at the root neck. The surface of the enamel, dentin and pulp were also developed based on average dimensions cataloged in the literature, while the supporting structures (spongy bone, cortical bone and periodontal ligament) were based on a buccolingual section image of the upper premolar region.

Geometry B, Figure 3b, was created from geometry A by editing the surface of the enamel and dentin to create a compartmentalized restoration region, to allow the insertion of the occlusal island (Figure 3d) over the cusps (under the occlusal load application areas). The maximum depth of the restoration region was 3.55 mm, below the 5 mm maximum depth for the use of composite resin of the bulk fill type (3M, 2020), to ensure at least 2 mm of pulpal roof. And, the diameter of the restoration was 6 mm, to enable the restoration to encompass two occlusal islands in cusps in the region of the occlusal contact points.

As for the occlusal island on the cusps, it was cylindrical, with a diameter of 2 mm and a height of 1 mm, within the minimum dimensions of the islands (VITA, 2020) and, to maintain the areas of occlusion applied in Poiate (2007), one with 0.85 mm² and another with 0.75 mm², to simulate occlusal contact with an antagonist tooth.

Geometry C, Figure 3c, was also created from geometry A, but with the editing of the enamel surface to allow the insertion of an occlusal island (Figure 3e) on the slope of a cusp supporting the tooth, but encompassing two regions of occlusal contact with areas similar to those of geometry A. With this, this geometry can represent the lower right 2nd premolar (tooth 45), that is, the tooth that occludes with tooth 15 or its antagonist, given the similarity of both teeth 15 and 45. Since the patent application by Vasconcellos et al. (2011) does not provide dimensions for the island over the cusp, the strategy adopted was to combine the minimum specification of the material to be used in this island of 1 mm depth and minimum width in the occlusal region (VITA, 2020) with the geometry outlined in the patent application. As the adhesive layer was not generated, the grooves were also not reproduced, however, a guide pin was added under the ridge of the island, as suggested by Vasconcellos et al. (2011).

From the constructed geometries, surface meshes were created with Tri3 triangular elements (1 face, 3 edges with 1 node at each end). The preference for this element was due to the complexity of the model geometries, since quadratic elements would present distortions capable of compromising the result.

To determine the size of the elements along the surfaces, an h-type refinement was used following the convergence studies of results carried out in Poiate (2006, 2007), resulting in elements ranging from 0.05 mm of edge (in regions of great curvature and small size) to 0.2 mm (in regions of small curvature and large size) in the same patterns to ensure similar accuracy.

Then, from the surface meshes (Tri3 elements), volumetric meshes of the Tet4 type were made (4 faces, 6 edges, 4 vertices and 1 node at each vertex). As in the previous step, the edges of these elements varied from 0.05 mm to 0.2 mm following the h-type refinements created. In evaluating the degree of distortion of the tetrahedral elements, less than 5% had an edge ratio greater than 3, as suggested by Cubit (2020).

From the geometries A, B and C, six models for the simulation were defined, as specified in Table 1, in which the differentiation was in the geometry, material and place of load application. The HC, RC and RICC models correspond to an upper right 2nd premolar (tooth 15), which is why they have the occlusal load on the cusps, and the models HV, RV and ICV correspond to a lower right 2nd premolar (tooth 45), so they have the occlusion load on the slope, i.e., they are antagonistic teeth.

The geometries were made in order to generate different models from a simple substitution of properties in the restoration sites. However, the HC model was not made using the same base geometry as the RC and RICC because the restoration involved part of the dentin. With this feature, it was not possible to just modify the properties of the elements of geometry B to represent a healthy tooth.

Geometry B could be used in the RC and RICC models, which simulate a class I restoration, because the difference between these models is only in the properties where the occlusal island was located on the cusps of the tooth. In the RC model, the entire restoration was made of resin and, in the RICC model, in the region of the occlusal contacts, there is a ceramic occlusal island, Figure 4.

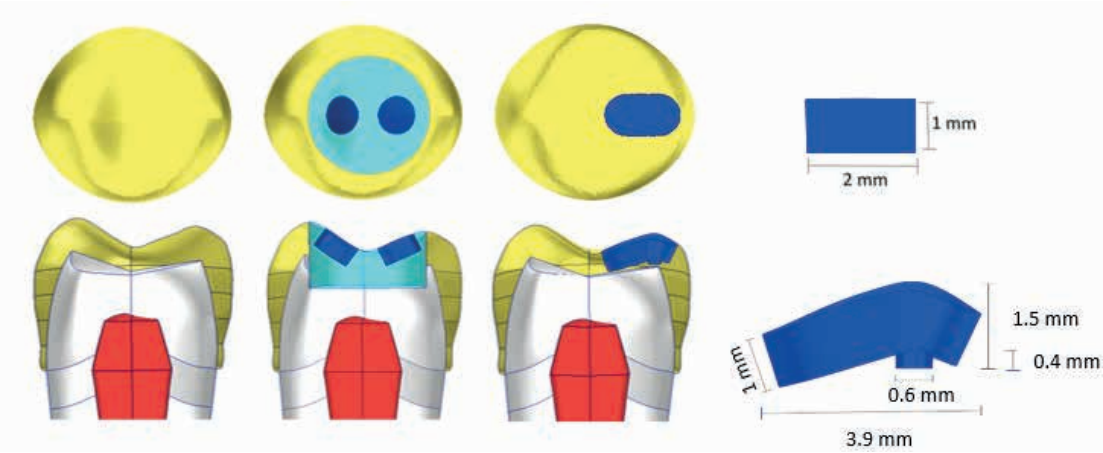

Figure 3: a)-c) Magnification in the region of differentiation of geometric models A, B and C in top and frontal views, d) Dimensions of the occlusal island of model B and e) of model C.

Geom. basis	Nodes	Elements	Differential characteristics	Acronym
A	178.426	1.031.818	Healthy in contacts	HC
B	183.521	1.045.554	Resin on contacts	RC
B			Resin with ceramic island on the contacts	RICC
C	189.722	1.097.463	Healthy on the slope	HV
C			Resin on strand	RV
C			Ceramic Island on the Strand	ICV

Table 1: Characteristics of the generated models and number of nodes and mesh elements.

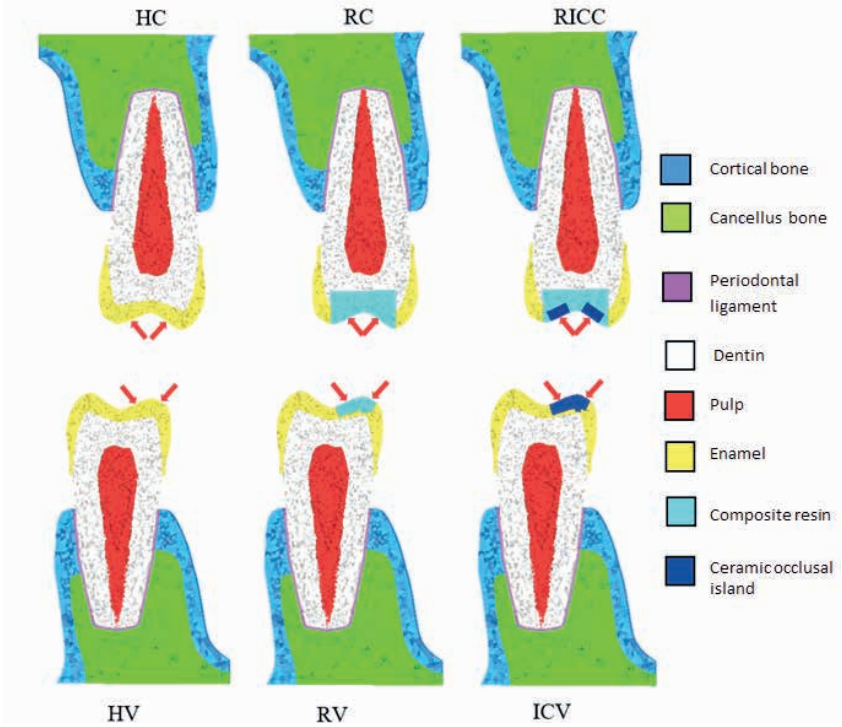

Figure 4: Buccal-lingual cross-section in the volumetric mesh of the six analysis models with indication of load application sites.

In turn, the HV, RV and ICV models were created by editing the properties of the occlusal island on the C geometry slope. While the HV island received enamel properties to represent a healthy tooth, the resin properties were given to the occlusal island of the RV model, and those of a ceramic were given to the ICV island.

The boundary conditions, also called fixation or bonding, are those determined for the edges or extremities of the modeled structures, so that it presents some support in space, with displacement and/or rotation restriction, to allow the analysis under the applied loads (BATHE, 1996 apud Poiate 2007).

In the six models, translational motion constraints in the x, y and z directions and rotational motion constraints in the x, y and z axes were used for the nodes on the mesial and distal surfaces of cancellous and cortical bone, as well as for the nodes on the surfaces of the maxillary sinus.

This same type of fixation condition was used by Poiate (2007) and, by Machado (2018) who restricted the displacement of the nodes present at the base and lateral side of the modeled cortical and spongy bone, while seeking to evaluate changes in the distribution of stresses in the presence of non-carious cervical lesions (NCCL) and different types of loading on an upper premolar. Huang (2020) modeled a smaller portion of the cortical bone, but maintained motion restriction in all directions for the lateral and inferior surface nodes of the set of supporting structures.

As for the loading condition, that is, the occlusal load due to masticatory efforts, Ferrario (2004) measured the maximum voluntary occlusion force on the second premolar of 36 men between 19 and 29 years old and obtained an average value of 291.36 N. on a second premolar in a homogeneous occlusion, with contact between all anterior teeth.

Yang (2018) used a load of 140 N on an upper premolar to simulate chewing by functional loads by MEF. However, Nishigawa et al (2001) verified that in episodes of nocturnal bruxism, the force of occlusion can exceed the maximum voluntary load. Thus, the maximum force of 291.36 N was applied in the simulated models.

In the HC, RC and RICC models, the mesh at the occlusal load application sites was about 0.2 mm, due to this, the load was distributed in 90 nodal points, 45 of which in an average area of 0.86 mm² on the buccal cusp and 45 in an area of about 0.92 mm² on the lingual cusp, Figure 34a.

In the HV, RV and ICV models, the mesh in the region of the load application slope was about 0.1 mm, so the force was distributed in 256 nodal points, 126 of which in an area of 0.92 mm² buccal cusp and 126 in an average area of 0.89 mm² in the lingual cusp. That is, in areas compatible with the dimensions of occlusal contact in premolars presented by Kumugai et al. (1999).

In all models, the loads were applied with an inclination of 45° in relation to the horizontal axis, with the resultant of 291.36 N parallel to the vertical axis of the tooth.

As in all types of numerical analysis, certain hypotheses need to be accepted in order to make the modeling process and problem solution viable. Therefore, all the constant structures in the model assumed an isotropic, homogeneous and linearly elastic behavior, characterized by two material constants, Young's modulus (E) and Poisson's coefficient (n), except for enamel, in which isotropy was maintained only in the horizontal axes (POIATE, 2006, 2007). Table 2 lists the values applied to each of these structures as well as their respective references.

For the RC, RICC and RV models, it was decided to use the mechanical properties of

Structure/Material	Young's Modulus (GPa)	Poisson Coefficient	Reference
Pulp	0.02	0.45	Farah e Craig (1974) apud Poiate (2007)
Dentin	18.6	0.31	Ko *et al.* (1992) apud Poiate (2007)
Enamel	E_{11} $E_{33}=E_{22}$	$v_{12}= v_{13}$ v_{23}	Niu *et al.* (2018)
	71.7 69.2	0.303 0.248	
Periodontal ligament	0.0689	0.45	Weinstein. Klaawitter e Cook (1980) apud Poiate (2007)
Cortical bone	13.7	0.3	Veiga (1996) apud Poiate (2006)
Cancellous bone	1.37	0.3	Veiga (1996) apud Poiate (2006)
Vita Enamic	37.4	0.206	Belli *et al.* (2017)
Filtek bulk fill posterior	15.6	0.3	Nabawy (2017)

Table 2: Mechanical properties of anatomical structures and materials in the models.

Material	Tensile strength (MPa)	Compressive strength (MPa)	Shear strength (MPa)	Reference
Adhesive Vita Adiva F-CEM	-	-	22	Vita (2020)
Vita Enamic ceramics	18.86	370	15.4	Elsaka (2014) / Kok et al (2014) / Belli et al (2017)
Dentin	103	282	138	Tanaka et al. (2003) / O'Brien (1997) apud Poiate (2006)
Enamel	16.7	321	90.2	Tanaka et al. (2003) / O'Brien (1997) apud Poiate (2006)
Filtek bulk fill posterior resin	35.5	213.4	20.34	Mandava et al (2017) / Azmi et al (2017) / Casanova (2018)

Table 3: Tensile, compression and shear strength of materials.

the composite resin Filtek bulk fill posteriorly measured by nanoindentation test, due to greater reliability in relation to the other tests.

As material for the occlusal island, it was decided to use glass-ceramic infiltrated with Vita Enamic resin in relation to nano-ceramic resin Lava Ultimate due to its better mechanical properties and, among the different tests that characterized it, the resonant beam was chosen, due to its greater reliability in relation to the other tests.

The interfaces between the anatomical structures and the other interfaces, such as the ceramic island x restoration and enamel/dentin x restoration, were assumed to be perfectly united, despite knowing that there was an adhesive layer used to adhere the materials. Such an adhesive layer was not created due to its negligible thickness and its lack of properties compared to other materials, such as cohesion and friction angle. The polymerization shrinkage of the modeled resin (bulk fill type) was also not considered.

The program used for analysis was MSC. Nastran (MSC Software, USA), version 2017, on an Intel Core i7 microcomputer with a 2.9 GHz processor, 1 TB hard disk and 8 Gb of RAM. The MSC.Patran program version 2017.0.1 (MSC Software, USA) used in pre-processing was also used in post-processing to visualize and evaluate the results.

The distribution of stresses, strain and displacements in the analyzed models was comparatively evaluated through plotting both as a color map in the models (isocamps) and in graphic form in the regions of interest and the results were compared with the resistance values (tensile stress, compression, shear) in the interfaces and in the modeled structures (Table 3) to assess whether such loads are potentially harmful to them.

Two interesting aspects in Table 3 are that both the Vita Enamic hybrid ceramic and the Filtek bulk fill resin have higher tensile strength than enamel (from 1.13 to 2.13 times), but when it comes to shear strength, they are much lower (from 4.43 to 5.86 times).

RESULTS AND DISCUSSIONS

In the models of the maxillary 2nd premolar (tooth 15), the sites with the highest values of von Mises stress are naturally located under the areas of occlusal load application, Figure 5. In the remaining enamel of the RC and RICC models, there was a subtle increase in von Mises stress when compared to the same areas of the HC model. However, in the area between the occlusal load application zones, the stresses in the RC and RICC models were lower than those in the HC. However, for materials with ductile behavior, in the RC model, in the load application zones, stresses above the tensile strength limit of the Filtek resin (35.5 MPa) occur. In the RICC model, in the valley between cusps, the stresses are above the tensile strength of the resin. Therefore, with a load of 291.36 N, damage to the restoration of the tooth could already begin. However, it is worth mentioning that the Filtek resin, as well as the Vita Enamic ceramic, are composite materials, so the application of other specific failure criteria for these types of materials would be more appropriate.

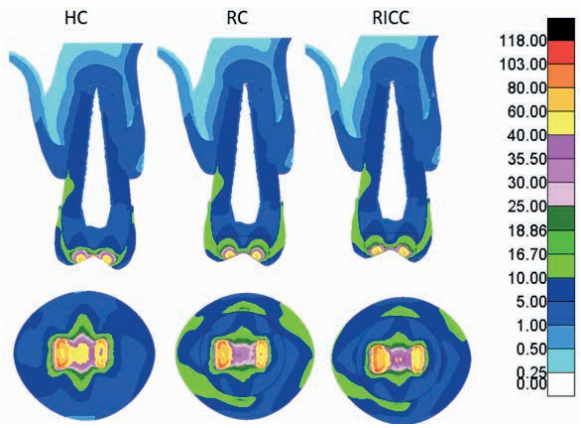

Figure 5: von Mises stress (MPa) in HC, RC and RICC (sectional and top views).

The HV, RV and ICV models (tooth 45) showed similar results, Figure 6, there was only a slight increase in von Mises tension around the occlusion load application region in RV and ICV, compared to HV, but between the load application sites, the tension was lower. When comparing the RV with the ICV, the RV model showed higher stress zones between 4 and 8 MPa in the region with enamel compared to the ICV. It is worth mentioning that in the three models the only difference was in the properties attributed to the occlusal island in slope, which despite the significant difference in Young's modulus between enamel and ceramic (about 1.9 times) and between enamel and resin (about 4.6 times), had little influence on the results, probably due to its dimensions and its positioning in relation to the occlusal load. There was no alteration in the other tooth support structures of the evaluated models.

However, the highest value found in the HV, RV and ICV models was about 1.36 times greater than that of the HC, RC and RICC models (2nd lower premolar, tooth 15), naturally due to the location of the applied load. For materials with ductile behavior, in the RV model, in the regions of occlusal load application, the stresses are above the tensile strength limit of the Filtek resin (35.5 MPa). Therefore, with a load of 291.36 N, damage could already begin in the restoration with this material on the tooth.

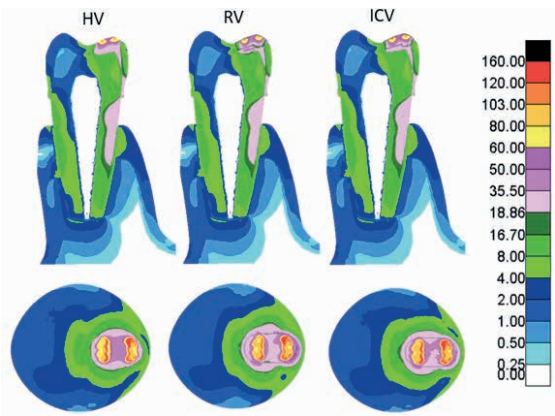

Figure 6: von Mises stress (MPa) in HV, RV and ICV (sectional and top views).

For maximum principal stress, positive values on the color scale indicate areas under tension, while negative values indicate compression. As observed in the von Mises stress, the remaining enamel of the RC and RICC models showed a maximum principal stress value above the healthy model (HC), but the stress between the load application areas of this model was higher than that of the RC and RICC, Figure 7. Between the RC and the RICC, the model without the occlusal island (RC) showed a slightly larger area between 8 and 16.7 MPa, indicating greater tensile stress in the tooth remaining compared to the RICC.

The interface zones between the enamel and the bulk fill restoration also showed sudden stress changes, mainly in the mesial and distal regions of the tooth, due to the difference in the materials' Young's modulus and the size of the restoration in the RC and RICC models. The highest compression values, in turn, were recorded in the load application areas. In the other tooth support structures of the evaluated models, there was no alteration in the stress distribution of the evaluated models.

In the RC and RICC models, in the region between the application of occlusal loads, there is a maximum principal stress greater than 35.5 MPa, exceeding the tensile strength limit of the resin (35.5 MPa). Similarly, in the HC model, in the region between the application of occlusal loads, the stresses are above the enamel tensile strength limit. Therefore, with a load of 291.36 N, damage to the healthy dental element (HC) would already begin.

Thus, these results show a beneficial effect in the use of the occlusal island for the recovery of regions in occlusal contact on cusps of the 2nd maxillary premolar injured by centric bruxism.

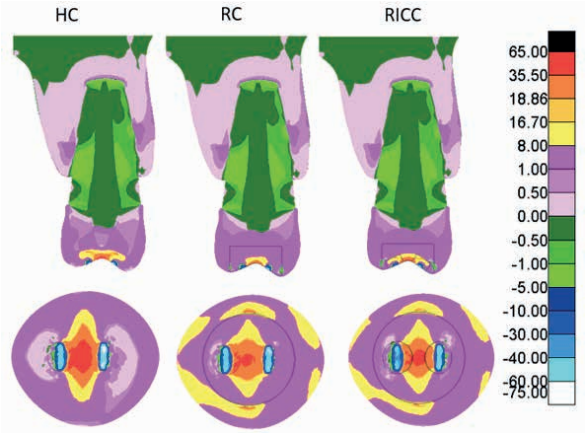

Figure 7: Maximum principal stress (MPa) in HC, RC and RICC (section and top view).

For the maximum principal stress between the HV, RV and ICV models, the RV was the one that presented the largest zones under tension above 18.86 MPa. In the ICV model, its stress areas above 8 MPa are more significant than in the healthy tooth (HV), Figure 8. In the cement-enamel junction of HV, RV and RICC, an increase in the area under tensile stress and in its intensity is verified in relation to the models of tooth 15, but below the enamel tensile strength limit of 16.7 MPa.

In the HV model, at the locations above and below the occlusal load application zones, a maximum principal stress above the tensile strength of the enamel is verified. Therefore, with a load of 291.36 N, damage to the tooth could already begin.

In the RV and ICV models, in the locations above and below the occlusal load application zones, there is a maximum principal stress above the tensile strength of the Vita Enamic ceramic. However, this result shows a beneficial effect in the use of the occlusal island for the recovery of regions in occlusal contact on the slope of the 2nd lower premolar injured by centric bruxism, since in the event of future failure of the occlusal island, it can be replaced with minimal damage to the remaining enamel.

Comparatively, the occlusal island on the side of the tooth is to a carbide insert, just as the enamel is to a cutting tool that supports the carbide insert, that is, with the wear of the occlusal island (carbide insert), it is enough to replace it, maintaining the structure of the enamel (support cutting tool). Therefore, the occlusal island functions as a sacrificial element, preserving the other structures, while a definitive solution is not available for the patient's centric bruxism.

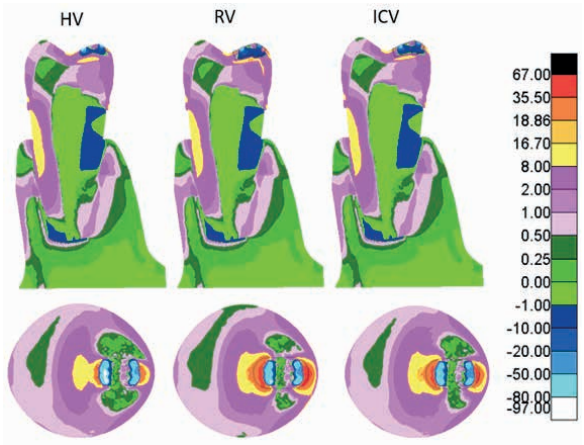

Figure 8: Maximum principal stress (MPa) in HV, RV and ICV (section and top views).

For the maximum shear stress in the HC, RC and RICC models, the highest values were located at the load application points of the model, reaching values greater than 50 MPa, Figure 9. Observing the remaining enamel of the models, the RC enamel shows the highest stress among the three, with a tension area between 5 and 10 MPa greater than that of the RICC, followed by the HC. However, the area between the load application points had a higher value in the HC, followed by the RICC and, finally, the RC.

As well as the von Mises stress and the main maximum, the RC and RICC models also showed a change in the maximum shear stress at the resin/enamel interface, jumping from a value between 2 and 5 MPa in the restoration to between 5 and 10 MPa on the mesial and distal face, due to the change in the properties

of the structures.

The maximum shear stress in the HC enamel remained below the shear strength of the enamel (90.2 MPa), while in the RC, in the occlusal load application zone, it exceeded the shear strength of the posterior Filtek bulk fill resin (20.34 MPa). In the RICC, the shear stress exceeded the shear strength of Vita Enamic (15.4 MPa) in the load application region and reached a shear stress above 20.34 MPa in the region between cusps (in the posterior bulk fill Filtek). In the buccal-lingual section in the HC, RC and RICC models, it can be seen that below the occlusal loading regions, the tension area between 5 and 10 MPa is greater in RC and RICC than in HC.

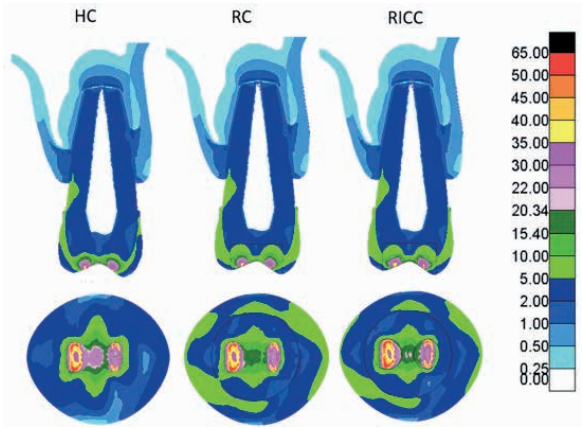

Figure 9: Maximum shear stress (MPa) in HC, RC and RICC (section and top view).

For the HV, RV and ICV models, the maximum shear stress was located in the areas where the load was applied, reaching values above 70 MPa. Among these zones, the HV model had the highest stress, followed by the ICV and RV, Figure 10. In the mesial and distal region of the outer enamel surface, as well as on the buccal cusp, the RV model showed areas with lower stress than the ICV and HV models. However, the island x enamel interface in the lingual region of the RV model was the most stressed among the three, followed by the ICV and the corresponding region of the HV. In the buccal-lingual section plane in the HV, RV and ICV models. A similar pattern of stress dissipation is verified along the tooth of the three models, however, in RC, at the resin/dentin interface, stresses between 20.34 and 22 MPa are observed, which is higher than in the other models.

As in the HC model, the shear stresses observed on the HV model did not exceed the enamel shear strength. Similarly, the stresses in the load application zones of the RV model exceeded the shear strength of the posterior bulk fill Filtek resin (20.34 MPa). In the ICV, the region between islands presented values higher than the shear strength of the material at that location (Filtek bulk fill posterior), while the regions where the occlusal load was applied exceeded the shear strength of 15.4 MPa of Vita Enamic.

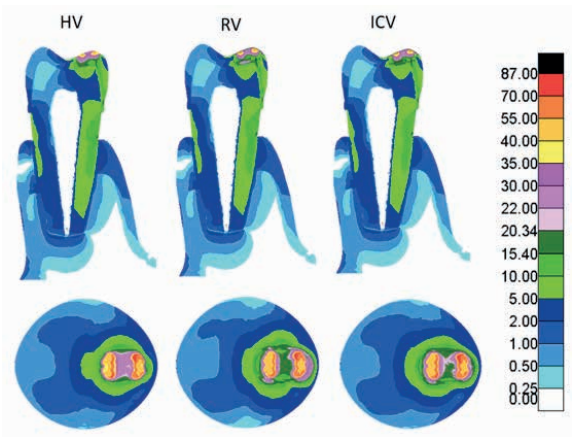

Figure 10: Maximum shear stress (MPa) in HV, RV and ICV (section and top view).

As for the results at the interfaces, the vertical axis indicates the value of the stresses in MPa, while the horizontal axis was dimensionless, which is why it alludes to the position of the node observed in relation to the face of the second premolar, ranging from 0 to 1, in which the interface located on the buccal surface is located at 0 and at 1, the distal at 0.25, the lingual at 0.5 and the mesial at 0.75. It is worth noting that for tooth 45, the distal and mesial faces are inverted in relation to tooth 15.

Figure 11a compares the maximum principal and shear stress at the restoration/enamel interface for RC and RICC (tooth 15). At the Filtek bulk fill x enamel restoration interface, the maximum principal stress had a higher peak value in the RC model (14 MPa) compared to the RICC (13 MPa). When comparing the other values, the RC presented zones with more intense tensile stress than the RICC on the mesial and distal faces, these faces where the highest stresses were recorded. In the lingual and buccal, the RICC model was the most tensile stress.

As with the maximum principal stress, on the faces with the highest stress (distal and mesial), the Filtek bulk fill x enamel restoration interface of the RC model was more loaded than that of the RICC. On the faces with less loading (lingual and buccal), the RICC presented higher values than the RC, Figure 11b.

When comparing the maximum principal stress obtained on the island x enamel interface nodes of the RV and ICV models (tooth 45), the RC interface showed the same behavior as the ICV, however, its values were higher than those captured in the ICV. While the peak of the ICV was around 35 MPa, the RV registered a maximum above 50 MPa, Figure 12a. For the shear stress of the island x enamel interface of the RV and ICV models, the results were similar on the buccal surface, however, on the lingual surface, the RV peak was above 30 MPa, while the ICV recorded values below 25 MPa, Figure 12b.

Comparing the results obtained with the studies by Yang et al. (2018), who sought to analyze the stress distribution in premolars with inlays and onlays restorations, modeled the external portion to the gingiva of a premolar restored with different materials such as e.max CAD ceramics, composite resin and gold alloy. After carrying out a static analysis in FEM, they verified that in models with composite resin, the remaining enamel showed values of maximum principal stress and von Mises higher than the same locations in models with ceramic restoration. This result corroborates those obtained in this work, since the maximum principal and von Mises stresses observed in the remaining enamel of the model without island (RV) were higher than those found in the model with island in Vita Enamic ceramic (ICV).

To verify the clinical performance between Class 1 restorations in direct composite resin and in indirect composite microceramics in a posterior tooth under occlusal contact zone, Shikder et al. (2019) followed 36 restorations in 18 patients over 12 months and compared the two restoration groups based on marginal adaptation and the presence of secondary caries. The study concluded that there was no statistically significant difference ($p>0.05$), because of the 18 resin restorations, only 2 failed at the restoration/enamel interface, while of the 18 ceramic restorations, only 1 failed. Thus, the significant reduction in maximum principal and shear stress on the island/glaze interface, observed in the ICV model (island on slope with Vita Enamic) compared to the RV (island on slope with Filtek bulk fill) could not be of practical relevance in the first 12 months. However, volunteers in the study by Shikder et al. (2019) did not have centric bruxism.

Sarapultseva and Sarapultsev (2019) obtained the same result as Shilkder et al. (2019) in another clinical study carried out on Class 1 restorations in posterior teeth analyzed for 24 months, with 27 restorations with direct composite resin in nanoceramics and 27 with direct composite resin bulk fill. At the end of the period, the two groups had similar survival rates, but the volunteers in the study also did not have centric bruxism and both restorations were direct.

Huang et al. (2020) analyzed by FEM the distribution of maximum principal stresses on

a premolar restored with three different CAD/CAM materials, such as IPS e.max CAD, Vita Enamic and Lava Ultimate under a load of 300 N along two occlusal contact zones close to the valley between tooth cusps. Thus, as in the RICC model of this work, the area under tensile stress in the model by Huang et al. (2020) which had the highest value of maximum principal stress was located in the valley between cusps, reaching 52 MPa. The RICC model presented a value between 30 and 50 MPa in this location, however, while the restoration of Vita Enamic modeled by Huang et al. (2020) encompassed all the cusps of the premolar (inlay), in the RICC model of this work, the Vita Enamic was located only in the islands under the occlusal contact region, while the valley between the cusps was recovered with the posterior Filtek bulk fill resin. By observing the occlusal contact region, the model by Huang et al. (2020) recorded stresses of -59 MPa, similar to those found in the same region of the RICC, between -40 and -60 MPa.

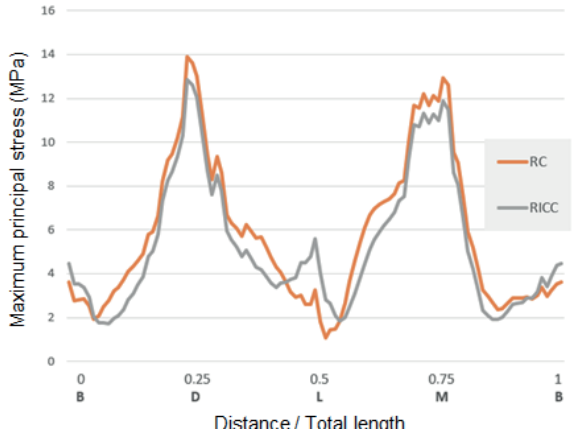

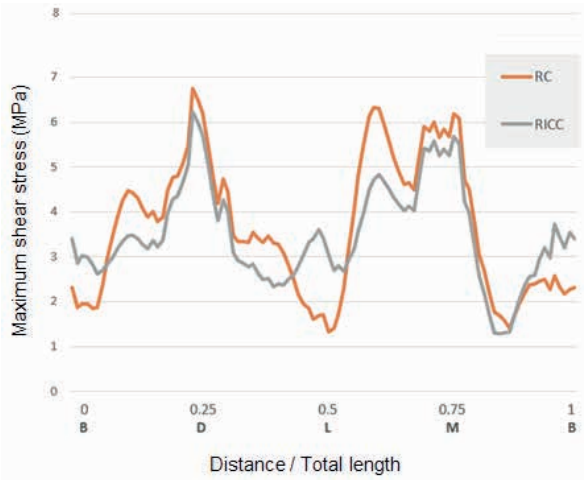

Figure 11: a) Maximum principal stress, b) Maximum shear stress (MPa) at the restoration x enamel interface in RC and RICC.

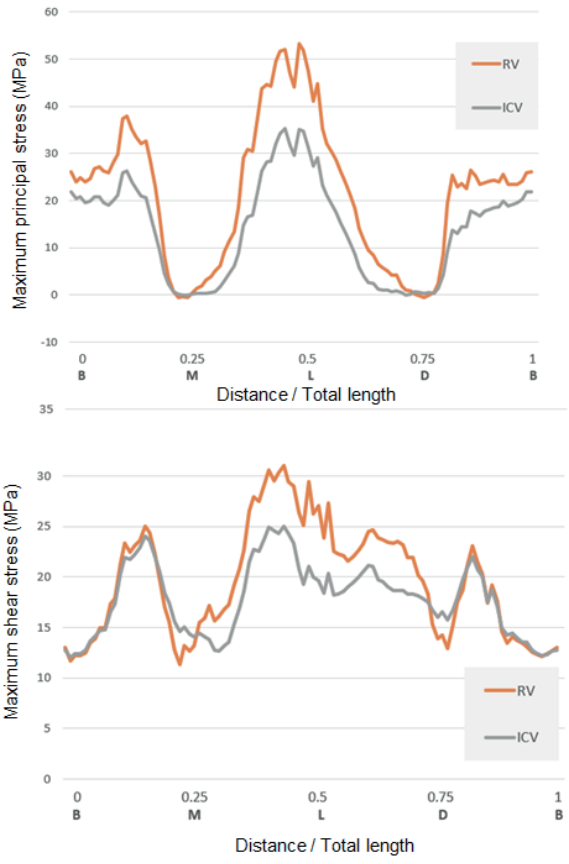

Figure 12: a) Maximum principal stress, b) Maximum shear stress (MPa) at the restoration x enamel interface in RV and ICV.

CONCLUSIONS

Based on the analysis of the results of the FEM simulation of the centric bruxism load applied to the upper and lower 2nd premolars, it is concluded that in Class I restorations, the use of an occlusal island made of Vita Enamic hybrid ceramic on cusps and housed in Filtek bulk fill resin, or the use of an occlusal island in an inclination, can have a beneficial effect on the longevity of the dental restoration in regions in occlusal contact injured by centric bruxism when the dental element is the 2nd premolar tooth. top or bottom, respectively. Therefore, the occlusal island can function as a sacrificial element, preserving the other structures, while there is no definitive solution for the patient's centric bruxism.

Furthermore, the use of an occlusal island made of Vita Enamic hybrid ceramic on cusps and housed in Filtek bulk fill resin on the upper 2nd premolar:

- Reduces von Mises stress, shear stress and tensile and compressive loads generated in the remaining enamel;
- Increases von Mises and shear stress between islands;
- Reduces the maximum principal and shear stress values of the restoration x enamel interface;
- Minimally reduces the intensity of maximum principal and shear stress on the enamel x dentin interface.

And, the use of an occlusal island in Vita Enamic hybrid ceramic in a mandibular 2nd premolar strand.

- Minimally increases the shear stress and compressive loads imposed on the remaining enamel;
- Reduces von Mises tension and tensile loads imposed on the remaining enamel;
- Reduces the maximum principal and shear stress on the island x enamel interface;
- It does not generate significant changes in the enamel x dentin interface.

REFERENCES

3M, **Filtek one resina bulk fill**. Perfil técnico do produto. 3M. 28 f. 2020.

ÁSTVALDSDÓTTIR, A. et al. **Longevity of posterior resin composite restorations in adults** – A systematic review. Journal of Dentistry, v. 43, p. 934-954, mai. 2015.

AZIMI, M. M. A. et al. **An in-vitro evaluation of mechanical properties and surface roughness of bulk fill vs incremental fill resin composites**. Internacional Journal of Preventive and Clinical Dental Research, v.4, n.1, p. 37-42, jan. 2017.

BARTLETT, D.; SUNDARAM, G. **As up to 3 year randomized clinical study comparing indirect and direct resin composites used to restore worn posterior teeth**. International Journal of Prosthodont, v. 19, n. 6, nov./dec. 2006.

BELLI, R. et al. **Chairside CAD/CAM materials. Part 1:** Measurament of elastic constants and microstrutural characterization. Dental Materials, v. 33, p. 84-98, out. 2017.

CASANOVA, Y. J. C. **Estudio comparativo in vitro de la resistência al cizallamiento de la resina compuesta nanotecnológica filtek bulk fill com fotopolimerizacion continua y discontinua en el ano 2018**. 90 f. Tese (Graduação em cirurgião dentista) – Universidad Alas Peruanas, Ica, 2018.

CESAR, Paulo. **Cerâmicas odontológicas**, 2006. Disponível em:

<https://edisciplinas.usp.br/pluginfile.php/321282/mod_resource/content/0/2-Cer%C3%A2micas-2006-Texto-Colunas.pdf >. Acesso em 06 maio 2020.

CHANTRE, D. T. **Hábitos parafuncionais e suas consequências na saúde oral**, 2019. 59 f. Tese (Mestrado em Medicina Dentária) – Instituto Universitário Egas Moniz. Portugal, Almada. 2019.

CUBIT. **Metrics for tetrahedral elements**. Disponível em: < https://cubit.sandia.gov/public/14.1/help_manual/WebHelp/mesh_generation/mesh_quality_assessment/tetrahedral_metrics.htm>. Acesso em: 06 mai 2020.

DEMJAHA, G. et al. **Bruxism unconscious oral habit in everyday life.** Macedonian Journal of Medical Sciences, v. 7, n. 5, p. 876-881, mar. 2019.

DUTRA, L. C. **Lesões dentárias oriundas da oclusão.** Revista da Universidade Vale do Rio Verde, Três Corações, v. 14, n. 1, p. 44-52, jan./jul. 2016.

ELSAKA, S. E. **Bond Stregth of novel CAD/CAM restorative materials to self-adhesive resin cement:** The effect of surface treatments. The Journal of Adhesive Dentistry, v.16, n.6, p. 531-540, aug. 2014.

FERRARIO, V. F. et al. **Single tooth bite forces in health young adults**. Journal of Oral Rehabilitation, v. 31, p.18-22, 2004.

GRACIS, S. et al. **A new classification system for all-ceramic and ceramic-like restorative materials**. The International Journal of Prosthodontics, v.28, n.3, 2015.

HUANG, X. et al. **Estimation of stress distribution and risk of failure for maxillary premolar restored by occlusal veneer with diferente CAD/CAM materials and preparation designs**. Clinical Oral Investigations, fev. 2020

KOK, P. et al. **Mechanical performance of implant-supported posterior crowns**. The Journal of Prosthetic Dentistry, v. 114, n. 1, p. 59-66, mar. 2015.

KUMUGAI, H. et al. **Occlusal force distribution on the dental arch during various levels of clenching**. Journal of Oral Rehabilitation, v. 26, p. 932-935, 1999.

LUDOVICHETTI, F. S. et al. **Wear resistance and abrasiveness of CAD-CAM monolithic materials**. The Journal of Prosthetic Dentistry, v. 120, ago. 2018.

MACHADO, A. C. et al. **Influência do desequilíbrio oclusal na origem de lesão cervical não cariosa e recessão gengival:** Análise por elementos finitos. Revista Odontológica do Brasil Central, n. 27, p. 83, p. 204-210, 2018.

MACKERLE, J. **Finite element modelling and simulations in dentistry: a bibliography 1990–2003**. Department of Mechanical Engineering, Linkoping Institute of Tecnology, Sweden, v. 7, n. 5, p. 277-303, out. 2004.

MANDAVA, J. et al. **Microtensile bond strength of bulk-fill restorative composites to dentin**. Journal of Clinical Experimental Dentistry, v.9, n.8, p.1023-1028, abr. 2017.

MUCELIN, T. **Onlay: resina ou cerâmica?.** 2015. 52 f. Tese (Bacharelado em Odontologia) – Universidade Federal de Santa Catarina, Florianópolis, 2015.

NABAWY, A. A. **Mechanical properties of contemporary resin composites determined by nanoindentation**. Tanta Dental Journal, v. 14, n. 13, p. 129-138, jul. 2017.

NISHIGAWA K. et al. **Quantitative study of bite force during sleep associated bruxism**. Journal of Oral Rehabilitation, v. 28, p. 485-491, 2001.

NIU, H. et al. **Elastic properties measurament of human enamel based on resonant ultrasound spectroscopy**. Journal of the Mechanical Behavior of Biomedical Materials, v. 89, p. 48-53, 2019.

OSIEWICZ, M. A. et al. **Wear of direct resin composites and teeth: considerations for oral rehabilitation**. European Journal Oral Science, p. 1-6, 2019.

POIATE, I. A. V. P. **Análise da distribuição de tensões em modelos tridimensionais de um incisivo central superior, gerado a partir de tomografia computadorizada, sob diferentes magnitudes de carga:** método dos elementos finitos. 2006. 244 f. (Dissertação em Odontologia) – Universidade Federal Fluminense, Niterói, 2006.

POIATE, I. A. V. P. **Análise biomecânica de dentes restaurados com retentor intra-radicular fundido, com e sem férula**. 2007. 82 f. Tese (Doutorado em Odontologia) – Faculdade de Odontologia da Universidade de São Paulo, São Paulo, 2007.

POIATE, I. A. V. P. et al. **2D and 3D Finite element analysis of central incisor generated by computerized tomography**. Computer Methods and Programs in Biomedicine, v.104, p. 292-299, mar. 2011.

SARAPULTSEVA, M. e SARAPULTSEV A. **Flowable bulk-fill materials compared to nano ceramic composites for class I cavities restorations in primary molars: a two-year prospective case-control study**. Dentistry Journal, v. 7, n. 94, 2019.

SERAIDARIAN, P. I. et al. **Bruxismo:** Uma atualização dos conceitos, etiologia, prevalência e gerenciamento. Jornal Brasileiro de Oclusão, ATM e Dor Orofacial, v. 1, n. 4, p. 290-295, out./dez. 2001.

SHIKDER, et al. **Clinical evaluation of composite resin and indirect micro ceramic composite resin restorations in class I cavity of permanent posterior teeth**. International Journal Human Sciences, v. 3, n. 2, abr. 2019

VALJAKOVA, E. et al. **Contemporary dental ceramic materials, a review: Chemical composition, physical and mechanical properties, indications for use**. Macedonian Journal of Medical Sciences, v.6, n.9, p.1742 – 1755, sep. 2018.

VASCONCELLOS, A. B. et al, inventor; Universidade do Estado de São Paulo, Universidade Federal Fluminense, cessionário. **Restaurações odontológicas por meio de ilhas oclusais/proximais e por meio de pinos cilíndricos oclusais**. Brasil Carta patente PI 1104585-0. Set 2011.

VITA. **Vita enamic. Catálogo de instruções de processamento**. 32 f. 2020.

YANG, H. et al. **Stress distribution in premolars restored with inlay or onlays: 3D finite element analysis**. Journal of Advanced Prosthodontics, v.10, p. 184-90, Feb. 2018.